Angiotensin II Activates H^+-ATPase in Type A Intercalated Cells

Vladimír Pech,*† Wencui Zheng,†‡ Truyen D. Pham,* Jill W. Verlander,‡ and Susan M. Wall*§

*Renal Division, Department of Medicine, and §Department of Physiology, Emory University School of Medicine, Atlanta, Georgia; and ‡Division of Nephrology, Hypertension, and Transplantation, Department of Medicine, University of Florida College of Medicine, Gainesville, Florida; †V.P. and W.Z. contributed equally this work.

ABSTRACT

We reported previously that angiotensin II (AngII) increases net Cl^- absorption in mouse cortical collecting duct (CCD) by transcellular transport across type B intercalated cells (IC) *via* an H^+-ATPase– and pendrin-dependent mechanism. Because intracellular trafficking regulates both pendrin and H^+-ATPase, we hypothesized that AngII induces the subcellular redistribution of one or both of these exchangers. To answer this question, CCD from furosemide-treated mice were perfused *in vitro*, and the subcellular distributions of pendrin and the H^+-ATPase were quantified using immunogold cytochemistry and morphometric analysis. Addition of AngII *in vitro* did not change the distribution of pendrin or H^+-ATPase within type B IC but within type A IC increased the ratio of apical plasma membrane to cytoplasmic H^+-ATPase three-fold. Moreover, CCDs secreted bicarbonate under basal conditions but absorbed bicarbonate in response to AngII. In summary, angiotensin II stimulates H^+ secretion into the lumen, which drives Cl^- absorption mediated by apical Cl^-/HCO_3^- exchange as well as generates more favorable electrochemical gradient for ENaC-mediated Na^+ absorption.

J Am Soc Nephrol 19: 84–91, 2008. doi: 10.1681/ASN.2007030277

The cortical collecting duct (CCD) consists of principal and intercalated cells (IC; Figure 1) and contributes to the regulation of acid-base and fluid and electrolyte balance.[1] Within the CCD, most net Na^+ absorption occurs across principal cells through the epithelial Na^+ channel (ENaC).[2] In contrast, IC mediate secretion of OH^-/H^+ equivalents and net Cl^- absorption.[3,4] Within mouse CCD, IC are subclassified on the basis of the location of the H^+-ATPase and the presence or absence of the Cl^-/HCO_3^- exchanger anion exchanger 1 (AE1). Type A IC (A-IC) mediate H^+ secretion and express the H^+-ATPase on the apical plasma membrane and AE1 on the basolateral plasma membrane, whereas type B IC (B-IC) express the H^+-ATPase on the basolateral plasma membrane.[5] The apical plasma membrane of type B cells expresses pendrin, a Na^+-independent Cl^-/HCO_3^- exchanger encoded by *Slc26a4,* which mediates Cl^- absorption and secretion of OH^- equivalents, such as HCO_3^-.[4,6,7] The apical plasma membrane of non–A, non–B-IC expresses both pendrin and the H^+-ATPase[8]; however, this cell subtype is very rare in mouse CCD.[9]

Although the mechanism of Na^+ absorption has been elucidated in detail, the molecular mechanism(s) responsible for Cl^- transport are less well understood. Cl^- absorption occurs primarily through transcellular transport across B-IC with a small contribution of a paracellular, conductive flux.[3,4,10–12] Cl^- enters B cells, at least in part, through the apical Cl^-/HCO_3^- exchanger, pendrin, and likely exits the cells across the basolateral plasma membrane through a Cl^- conductance.[3,10] Within mouse CCD, we observed that angiotensin II (AngII) increases Cl^- absorption by transcellular transport across B-IC through a pendrin- and

Received March 6, 2007. Accepted July 27, 2007.

Published online ahead of print. Publication date available at www.jasn.org.

Correspondence: Dr. Vladimir Pech, Emory University School of Medicine, Renal Division, 1639 Pierce Drive, NE, WMB Room 338, Atlanta, GA 30322. Phone: 404-727-2797; Fax: 404-727-3425; E-mail: vpech@emory.edu

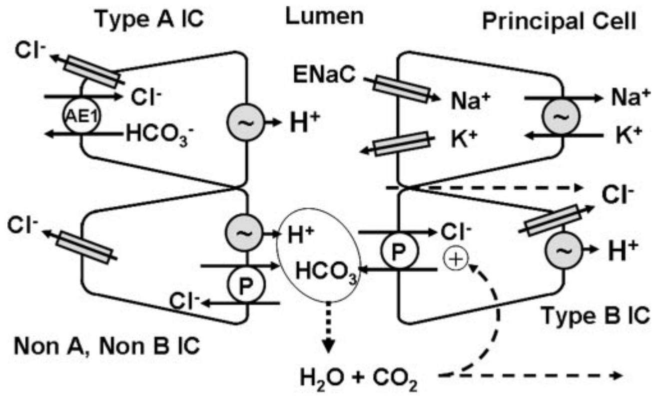

Figure 1. Ion transporters within the CCD. The CCD consists of principal cells (PC) and IC. PC mediate Na^+ absorption largely through an electrogenic, ENaC-dependent mechanism, thereby generating lumen-negative V_T, which drives paracellular Cl^- absorption. A-IC secrete H^+ by serial action of the apical H^+-ATPase and the basolateral Cl^-/HCO_3^- exchanger AE1. B-IC express a basolateral H^+-ATPase and the apical Cl^-/HCO_3^- exchanger pendrin. We propose that AngII activates the apical H^+-ATPase. The ensuing net H^+ secretion titrates luminal HCO_3^-. Thus, luminal HCO_3^- concentration falls, which increases the driving force for apical Cl^-/HCO_3^- exchange. CO_2 so generated further activates apical anion exchange. The result is increased Cl^- and HCO_3^- absorption. P, pendrin.

an H^+-ATPase–dependent mechanism[12]; therefore, we hypothesized that AngII either increases apical plasma membrane pendrin expression or increases the driving force for apical Cl^-/HCO_3^- exchange, such as by activating the H^+-ATPase. Because intracellular trafficking is a major mechanism by which both pendrin and the H^+-ATPase are regulated,[13–16] we asked whether AngII induces subcellular redistribution of pendrin and/or the H^+-ATPase. To answer this question, we performed immunogold cytochemistry and ion transport studies in mouse CCD perfused *in vitro*.

RESULTS

Within Type B Cells, AngII Does not Alter the Subcellular Distribution of Pendrin or the H^+-ATPase

We asked whether AngII application *in vitro* increases Cl^- absorption by increasing apical plasma membrane pendrin expression. To answer this question, CCD were perfused *in vitro* from mice given a NaCl-replete diet and furosemide for 5 d to upregulate pendrin, H^+-ATPase, and ENaC protein expression.[12,17–19] Pendrin expression was quantified in these tubules with immunogold cytochemistry. Numerous gold particles labeled the cytoplasmic vesicles of the B-IC, whereas only faint background staining was present in the cytoplasm of the adjacent principal cells (Figure 2). As shown (Figure 3, Table 1), a 45-min exposure to AngII did not increase apical plasma membrane pendrin expression in B cells. However, pendrin-mediated Cl^- absorption might increase through activation of the basolateral plasma membrane H^+-ATPase in B cells. Increased net H^+ efflux, such as through

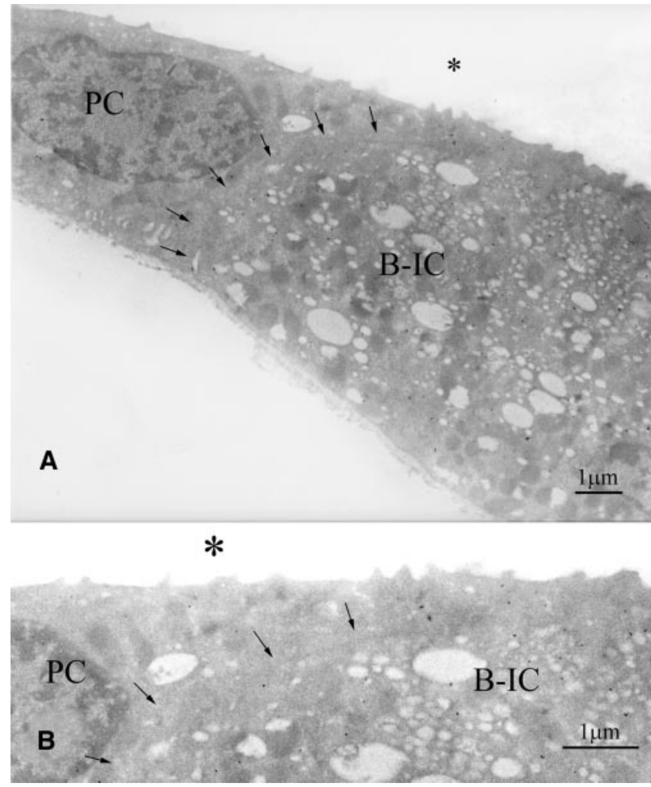

Figure 2. Pendrin immunolabel in B-IC and PC. Representative transmission electron micrographs of a control isolated perfused CCD labeled for pendrin by immunogold cytochemistry. (A) Low-magnification image illustrating B-IC on the right and PC on the left. Bar = 1 μ; *tubule lumen, arrows indicate lateral cell border. (B) Higher magnification image of the apical region of cells shown in A. Numerous gold particles label the cytoplasmic vesicles of the B-IC. Few gold particles are present in the cytoplasm of the PC.

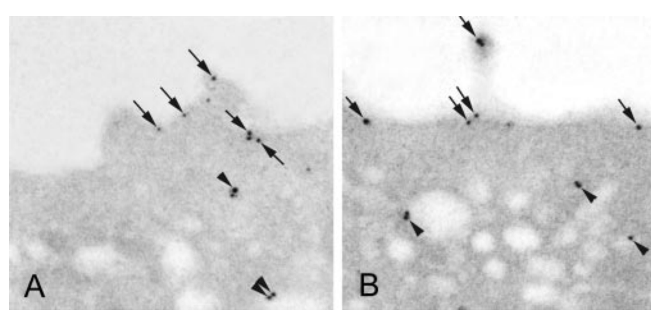

Figure 3. B cell pendrin immunolabel in the presence and absence of AngII. Representative transmission electron micrographs showing pendrin immunogold labeling in the apical plasma membrane (arrows) and apical cytoplasmic vesicles (arrowheads) in a B-IC under control conditions (A) and after a 45-min application of AngII (10^{-8} M) to the bath (B). AngII treatment produced no appreciable difference in cell structure or in pendrin distribution or abundance. These observations were verified by morphometric analysis and quantitative immunogold analysis (see Table 1).

activation of the H^+-ATPase, should raise intracellular HCO_3^- concentration, thereby augmenting the driving force for apical Cl^-/HCO_3^- exchange. Thus, basolateral plasma membrane H^+-

Table 1. Effect of AngII on cell morphometry and pendrin and H^+-ATPase subcellular distribution in B-IC[a]

B-IC	Pendrin		H^+-ATPase	
	Control (n = 3)	AngII (n = 4)	Control (n = 4)	AngII (n = 4)
Apical plasma membrane boundary length, μm	14.6 ± 2.6	13.5 ± 0.3	N/A	N/A
Apical plasma membrane immunolabel, gold particles/cell profile	24.9 ± 6.2	20.9 ± 5.0	N/A	N/A
Apical plasma membrane pendrin label density, gold particles/μm	1.66 ± 0.13	1.53 ± 0.33	N/A	N/A
Basolateral plasma membrane immunolabel, gold particles/cell profile	N/A	N/A	24.2 ± 7.5	28.2 ± 2.4
Immunolabel over the cytoplasm and cytoplasmic vesicles, gold particles/cytoplasm	249 ± 63	273 ± 53	141 ± 12	129 ± 11
Pendrin cytoplasmic label density, gold particles/μm^2 of cytoplasmic area	4.4 ± 0.7	4.6 ± 0.9	N/A	N/A
Pendrin subcellular immunolabel redistribution ratio, apical plasma membrane gold/cytoplasmic gold.	0.106 ± 0.021	0.078 ± 0.011	N/A	N/A
H^+-ATPase subcellular immunolabel redistribution ratio, basolateral plasma membrane gold/cytoplasmic gold.	N/A	N/A	0.178 ± 0.055	0.219 ± 0.008

[a] H^+-ATPase or pendrin protein abundance was determined by quantifying the number of immunogold particles directed at H^+-ATPase and pendrin antigen–antibody interactions, respectively. n = number of tubules studied. N/A, not applicable.

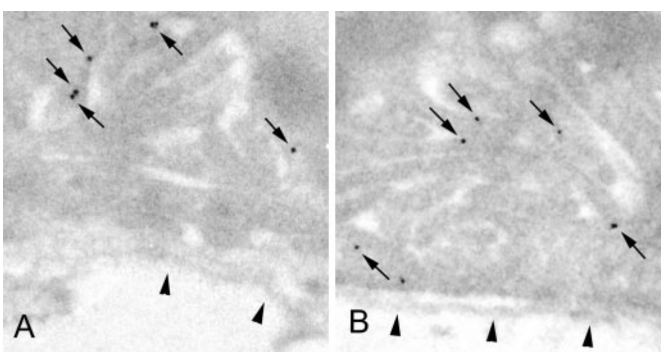

Figure 4. B cell H^+-ATPase immunolabel in the presence and absence of AngII. Representative transmission electron micrographs showing H^+-ATPase immunogold labeling in the basolateral plasma membrane (arrows) of B-IC under control conditions (A) and after a 45-min application of AngII (10^{-8} M) to the bath (B). AngII treatment produced no appreciable difference in H^+-ATPase distribution or abundance in B-IC; these observations were verified by quantitative immunogold analysis (see Table 1). Arrowheads point to the basement membrane.

ATPase expression in type B cells was quantified in the presence and absence of AngII. As shown (Figure 4, Table 1), basolateral plasma membrane H^+-ATPase expression was unchanged with AngII application. We concluded that within B-IC, AngII application *in vitro* does not alter the subcellular distribution of pendrin or H^+-ATPase.

AngII Regulates Intracellular Distribution of H^+-ATPase in A-IC

Activation of the apical plasma membrane H^+-ATPase should reduce luminal HCO_3^- concentration by titrating HCO_3^- to form CO_2 and water. When luminal HCO_3^- concentration falls, the driving force increases for B cell apical Cl^-/HCO_3^- exchange. Thus, we asked whether AngII increases apical plasma membrane H^+-ATPase expression within A-IC. As shown, with application of AngII to the bath, the proportion of H^+-ATPase expressed in the apical plasma membrane relative to the cytoplasm increased more than three-fold (Table 2, Figure 5). Only a few gold particles were present in the cytoplasm of the adjacent principal cells (Figure 6). We concluded that AngII increases apical plasma membrane H^+-ATPase expression in A-IC through subcellular redistribution.

AngII Stimulates HCO_3^- Absorption in CCD

We asked whether AngII increases H^+-ATPase expression and function in tandem. Thus, net HCO_3^- flux (J_{tCO2}) was measured in CCD perfused *in vitro* under conditions identical to the H^+-ATPase localization studies described. Under basal conditions, net HCO_3^- secretion was observed; however, with application of AngII, CCD absorbed HCO_3^- (Figure 7), which indicates increased secretion of H^+ equivalents. Thus, AngII activates net H^+ secretion in A-IC. We concluded that AngII enhances H^+ secretion, at least in part, by enhanced apical plasma membrane H^+-ATPase expression in A-IC.

DISCUSSION

We reported previously that AngII stimulates Cl^- absorption in the CCD of wild-type but not of *Slc26a4* null mice.[12] Thus, AngII-induced Cl^- absorption occurs through a pendrin-dependent mechanism. Whereas *in vivo* studies showed that

Table 2. Effect of AngII on cell morphometry and H^+-ATPase subcellular distribution in A-IC[a]

A-IC	Control ($n = 4$)	AngII ($n = 5$)
Apical plasma membrane boundary length, μm	19.3 ± 4.4	32.2 ± 4.2[b]
Apical plasma membrane H^+-ATPase label, gold particles/cell	13.9 ± 6.2	35.8 ± 8.3[b]
Apical plasma membrane H^+-ATPase label density, gold particles/μm	0.60 ± 0.20	1.11 ± 0.20
H^+-ATPase label over the cytoplasm and cytoplasmic vesicles, gold particles/cytoplasm	167 ± 34	177 ± 15
H^+-ATPase cytoplasmic label density, gold particles/μm^2 of cytoplasmic area	6.3 ± 1.0	7.4 ± 0.6
Subcellular H^+-ATPase label redistribution ratio, apical plasma membrane gold/cytoplasmic gold.	0.069 ± 0.025	0.210 ± 0.048[c]

[a]H^+-ATPase label was determined by the number of immunogold particles directed at H^+-ATPase antigen-antibody interactions. n = number of tubules studied.
[b]$P = 0.05$ to 0.10 *versus* control.
[c]$P < 0.05$.

chronic regulation of pendrin occurs mainly through subcellular redistribution between apical plasma membrane and cytoplasmic vesicles,[13,14] this study shows that AngII does not modulate Cl^- absorption through pendrin trafficking when applied *in vitro* at a concentration (10^{-8} M) observed in the cortical interstitium *in vivo*.[20] Therefore, AngII-stimulated Cl^- absorption must be achieved by other mechanism(s), such as through posttranslational modification of pendrin or through changes in the driving force for apical anion exchange. In this study, we observed that AngII increases apical plasma membrane H^+-ATPase expression in A-IC in tandem with increased HCO_3^- absorption (or increased net H^+ secretion). Because activation of the H^+-ATPase reduces luminal HCO_3^- concentration, the driving force for apical Cl^-/HCO_3^- exchange increases, thus increasing net Cl^- absorption. H^+-ATPase activation is critical in AngII-induced Cl^- absorption, because angiotensin does not alter Cl^- absorption when the H^+-ATPase is inhibited.§[12]

We cannot exclude the possibility, however, that AngII also activates B cell transporters, such as pendrin and the basolateral plasma membrane H^+-ATPase, through mechanisms other than trafficking, such as posttranslational modification. Moreover, AngII might increase the driving force for apical anion exchange by a direct effect on basolateral Cl^- exit from B cells, such as through changes in KCl co-transport[21] or changes in a basolateral Cl^- channel[22]; however, either primary or secondary activation of apical anion exchange in B cells by AngII should increase luminal bicarbonate concentration, which was not observed in this study. Instead, we observed reduced luminal HCO_3^- concentration with AngII application.

AngII activates the H^+-ATPase in the proximal tubule.[23] In more distal regions of the nephron, however, regulation of the H^+-ATPase by AngII remains particularly controversial. In the late distal tubule[24] and in distal nephron cells in culture (MDCK),[25] AngII activates the H^+-ATPase. In contrast, Tojo *et al.*[26] demonstrated a dosage-dependent inhibition of the H^+-ATPase by AngII in permeabilized CCD segments; however, Tojo *et al.* studied the H^+-ATPase activity in pooled membrane fragments. Therefore, possible effects of AngII on the subcellular distribution of H^+-ATPase could not be discerned.

The primary physiologic role of AngII is to maintain arterial blood pressure through vasoconstriction and by increasing renal Na^+ absorption, such as through ENaC activation in the CCD.[27] Because ENaC-mediated Na^+ absorption generates a current of positive charge from the lumen to the bath, we expected transepithelial voltage (V_T) to become more lumen negative with AngII. Instead, V_T did not change after application of the hormone.[12] Thus, movement of another ion must shunt the potential generated by ENaC-mediated Na^+ absorption. Electrogenic Cl^- absorption might shunt the V_T generated by ENaC; however, AngII-stimulated Cl^- absorption is largely mediated by pendrin, which is likely an electroneutral exchanger.[28,29] Although electrogenic K^+ secretion attenuates the voltage generated by this Na^+ current, Na^+ absorbed greatly exceeds K^+ secreted.[30] Thus, another ion current must shunt the electrical potential generated by ENaC-mediated Na^+ absorption. Because the vacuolar H^+-ATPase is an electrogenic transporter,[16,31,32] luminal H^+ secretion is a likely candidate. Simultaneous activation of apical plasma membrane H^+-ATPase and ENaC by AngII increases two currents in opposing directions. AngII application thus increases absorption of Na^+ and Cl^- and increases secretion of H^+ equivalents without an

§This study demonstrates that AngII activates the apical but not the basolateral plasma membrane H^+-ATPase; however, we observed previously that application of the H^+-ATPase inhibitor bafilomycin to the bath solution abolished AngII-stimulated Cl^- absorption.[12] Thus, stimulation of pendrin-dependent Cl^- absorption by AngII could be dependent on the basolateral plasma membrane H^+-ATPase. However, peritubular application might inhibit both the apical and the basolateral plasma membrane H^+-ATPase because bafilomycin is membrane permeable.[36] Thus, the effect of peritubular bafilomycin (10 nM) on AngII-stimulated J_{tCO2} was explored. If bafilomycin inhibits only H^+ efflux across the basolateral plasma membrane of B cells, then it should reduce intracellular HCO_3^- concentration, thereby attenuating apical anion exchange. The result would be reduced luminal HCO_3^- concentration and a more positive J_{tCO2}. In contrast, inhibition of H^+ secretion by A cells would increase luminal HCO_3^- concentration, thereby making J_{tCO2} less positive. We observed that in CCD perfused *in vitro* from furosemide-treated mice, J_{tCO2} was -0.1 ± 1.3 pmol/mm per min ($n = 6$) in the absence and -2.6 ± 1.3 pmol/mm per min ($n = 5$; $P = 0.17$) in the presence of bafilomycin in the bath solution. Thus, application of bafilomycin to the bath solution does not *reduce* HCO_3^- secretion. One explanation for these data is that peritubular bafilomycin inhibits both the apical and the basolateral plasma membrane H^+-ATPase. J_{tCO2}. In contrast, inhibition of H^+ secretion by A cells would increase luminal HCO_3^- concentration, thereby making J_{tCO2} less positive. We observed that in CCD perfused *in vitro* from furosemide-treated mice, J_{tCO2} was -0.1 ± 1.3 pmol/mm per min ($n = 6$) in the absence and -2.6 ± 1.3 pmol/mm per min ($n = 5$; $P = 0.17$) in the presence of bafilomycin in the bath solution. Thus, application of bafilomycin to the bath solution does not *reduce* HCO_3^- secretion. One explanation for these data is that peritubular bafilomycin inhibits both the apical and the basolateral plasma membrane H^+-ATPase.

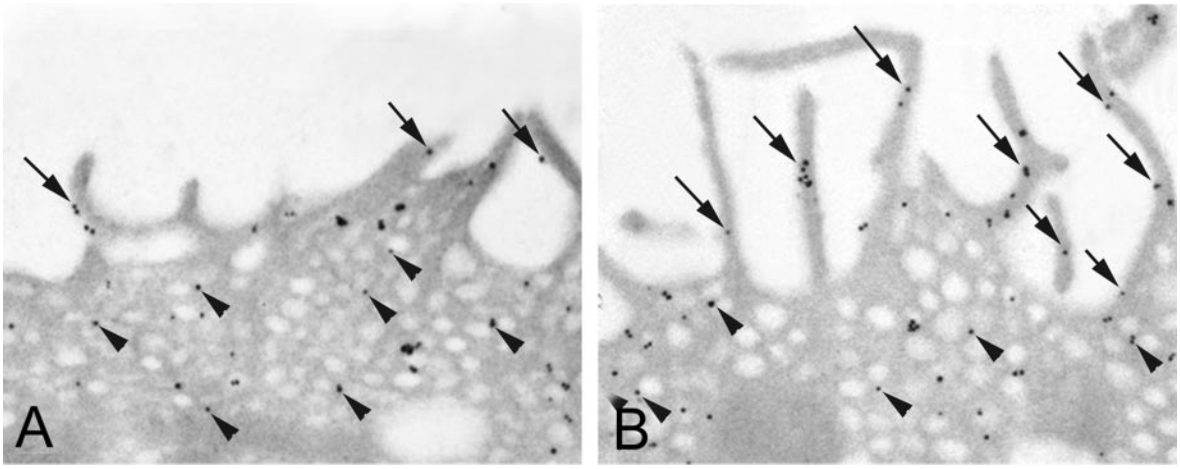

Figure 5. A cell H^+-ATPase immunolabel in the presence and absence of AngII. Representative transmission electron micrographs showing H^+-ATPase immunogold labeling in the apical plasma membrane (arrows) and apical cytoplasmic vesicles (arrowheads) in A-IC under control conditions (A) and after application of 10^{-8} M AngII to the bath (B). A-IC exhibited redistribution of the H^+-ATPase. H^+-ATPase abundance increased in the apical plasma membrane relative to the cytoplasmic vesicles, which was confirmed by quantitative immunogold analyses (see Table 2). As illustrated, an increase in the length and number of apical plasma membrane microprojections was observed in many type A cells in the AngII-treated tubules, although the difference in apical plasma membrane boundary length was not statistically significant (see Table 2).

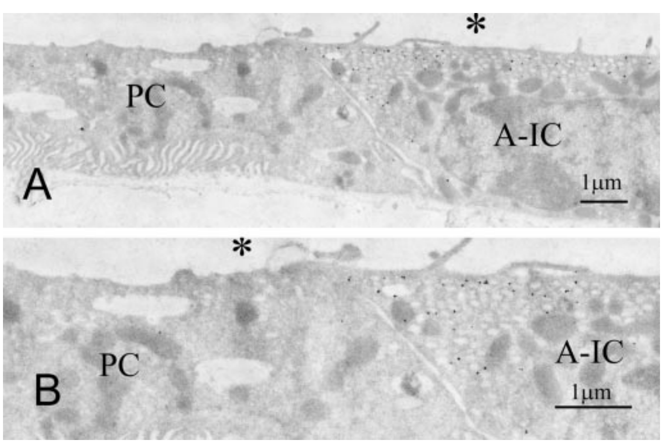

Figure 6. H^+-ATPase immunolabel in A cells and in PC. Transmission electron micrographs of a control isolated perfused CCD labeled for the H^+-ATPase by immunogold cytochemistry are shown. (A) Low-magnification image illustrating an A-IC on the right and PC on the left. Bar = 1 μ; *tubule lumen. (B) Higher magnification image of the apical region of cells shown in A. Numerous gold particles label the apical cytoplasmic vesicles and a few particles label the apical plasma membrane of the A-IC. Only rare gold particles are present in the cytoplasm of the PC.

appreciable change in V_T. These and previously published data are consistent with the hypothesis that the H^+-ATPase shunts the V_T generated by ENaC-mediated Na^+ absorption.‖

This and previous studies show a novel role of the apical H^+-ATPase in AngII-induced NaCl absorption in the CCD. We propose that the H^+-ATPase modulates NaCl absorption in this segment through three mechanisms. First, protons secreted by the H^+-ATPase titrate luminal HCO_3^- to produce H_2O and CO_2. Thus, luminal HCO_3^- concentration is reduced, which provides a more favorable driving force for apical Cl^-/HCO_3^- exchange-mediated Cl^- absorption.[33] Second, the CO_2 thus generated diffuses from the lumen into B cells, which further stimulates apical anion exchange.[34] Third, because the H^+-ATPase is an electrogenic transporter,[31,32] H^+-ATPase–mediated H^+ secretion should generate a more favorable electromotive force for ENaC-mediated Na^+ absorption. The blunted increment in net Cl^- absorption observed in CCD from *Slc26a4* null mice in response to AngII likely contributes to the reduced apparent vascular volume and lower BP observed in these mutant mice with furosemide administration or after dietary restriction of NaCl or Cl^- alone.[12,35]

Using mouse CCD perfused *in vitro*, we demonstrate that the regulation of pendrin and H^+-ATPase expression and function can be studied in native tissue *in vitro* under identical conditions. Moreover, this approach enables study of transporter trafficking without the changes in protein function that can occur with fluorescent tags.

We conclude that acute application of AngII *in vitro* increases apical plasma membrane H^+-ATPase expression and function specifically in A-IC. Activation of the apical plasma membrane H^+-ATPase reduces luminal HCO_3^- concentration, thus providing an active step for net Cl^- absorption. Moreover, H^+ secretion generates a more favorable electromotive force for ENaC-mediated Na^+ absorption. Thus, in

‖We observed previously that AngII does not change V_T in the CCD.[12] To test the hypothesis that the H^+-ATPase activation shunts the V_T generated by AngII-induced ENaC activation, we compared V_T measured in the presence and absence of bafilomycin reported previously.[12] In the presence of AngII alone, V_T was -2.2 ± 0.7 mV ($n = 16$).[12] With AngII plus bafilomycin in the bath, V_T was -8.0 ± 1.7 mV ($n = 6$; $P < 0.05$).[12] One explanation of these data is that in the absence of the H^+-ATPase–mediated proton secretion, the ENaC-mediated V_T is unmasked.

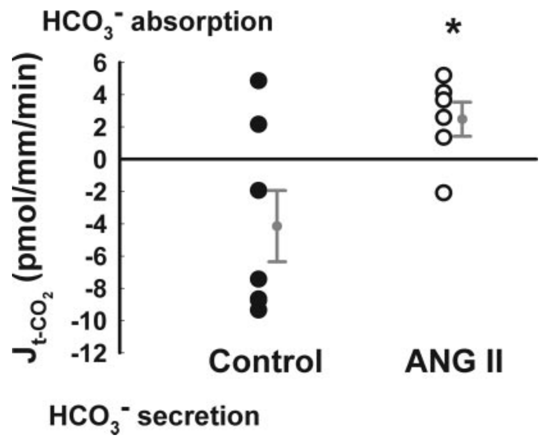

Figure 7. AngII reduces secretion of net OH^- equivalents in the CCD. The effect of AngII on J_{tCO2} was explored. Under basal conditions (●), CCD secreted HCO_3^- (J_{tCO2} = −4.2 ± 2.2 pmol/mm per min; *n* = 7), whereas peritubular application of AngII (10^{-8} M; ○) activated H^+ secretion, which resulted in HCO_3^- absorption (J_{tCO2} = 2.5 ± 1.1 pmol/mm per min; *n* = 6). In the absence of AngII, t_{CO2} concentrations in the perfusate and collected fluid samples were 24.5 ± 0.2 mM (*n* = 7) and 26.3 ± 0.8 mM, respectively ($P < 0.05$). In the presence of AngII, t_{CO2} concentrations in the perfusate and collected fluid samples were 25.2 ± 0.2 mM (*n* = 6) and 24.2 ± 0.6 mM, respectively (P = 0.09). *$P < 0.05$ *versus* control. Each circle represents a single tubule. Bars show means ± SEM.

addition to its widely known role in acid-base homeostasis, the H^+-ATPase plays a novel role in NaCl homeostasis. However, the extent to which H^+-ATPase activation contributes to ENaC-mediated Na^+ absorption remains to be determined. Moreover, whether the increased apical plasma membrane H^+-ATPase expression occurs in response to another signal, such as a reduction in intracellular pH (pHi) that results from increased H^+ uptake or increased HCO_3^- efflux across the basolateral plasma membrane, remains to be determined.

CONCISE METHODS

Animals

All experiments were performed on male and female wild-type mice (strain 129S6/SvEv; Taconic Farms, Germantown, NY). Mice were fed a balanced diet (53881300; Zeigler Brothers, Gardners, PA) prepared as a gel (0.6% agar, 74.6% water, and 24.8% mouse chow) supplemented with NaCl (approximately 1.13 mEq/d NaCl) plus furosemide (100 mg/kg per d) for 5 d to upregulate pendrin, H^+-ATPase, and ENaC expression in CCD.[12,17–19] All animal protocols were approved by the Emory University Institutional Animal Care and Use Committee.

In Vitro Perfusion of Isolated CCD

CCD were dissected from medullary rays and perfused at flow rates of 2 to 3 nl/min per mm in the presence of symmetric, physiologic solutions containing (in mmol/L) 125 NaCl, 2.5 K_2HPO_4, 24 $NaHCO_3$/5% CO_2, 2 $CaCl_2$, 1.2 $MgSO_4$, and 5.5 glucose bubbled with 95% air/5% CO_2.[6,35] Tubules were equilibrated at 37°C for 30 min before the collections were started. Tubules were perfused in the presence and absence of AngII (10^{-8} M) applied to the bath and/or bafilomycin A1 applied to the bath (10^{-8} M). Stock solutions of AngII (10^{-5} M) and bafilomycin (10^{-5} M) were prepared in deionized water and in absolute ethanol, respectively. All chemicals were purchased from Sigma-Aldrich (St. Louis, MO).

Measurement of J_{tCO2}

Total CO_2 (HCO_3^- + H_2CO_3 + CO_2) concentration was measured in perfusate and collected samples using a continuous-flow fluorimeter using the method of Zhou *et al.*[37] Transepithelial total CO_2 flux, J_{tCO2}, was calculated according to the equation $J_{tCO2} = (C_0 - C_L)Q/L$, where C_0 and C_L are the ion concentrations measured in the perfusate and collected fluid, Q is flow rate in nl/min and L is tubule length. Net fluid transport was taken to be zero because net fluid flux has not been observed in CCD when perfused *in vitro* in the presence of symmetric solutions and in the absence of vasopressin.[38–40] J_{tCO2} was expressed in picomoles per millimeter per minute. In each tubule studied, measurements were made under only a single experimental condition.

Fixation of Tubules Perfused In Vitro

Separate tubules were studied in flux and immunogold cytochemistry experiments. CCD were perfused *in vitro* as indicated previously with or without AngII in the bath for 45 min at 37°C, which represents the midpoint at which collections were made, and then fixed. To do so, both perfusate and bath were quickly exchanged for fixative, which contained the perfusate solution and 1% glutaraldehyde. Tubules were then disconnected from the pipettes and transferred into a glass well and incubated in fixative for 1 h at 4°C. Tubules were then trapped in 2% agar and immersed in PBS (pH 7.4), stored at 4°C, and shipped overnight on ice to the University of Florida College of Medicine Electron Microscopy Core Facility.

Tubule Processing and Immunogold Localization

The preserved tubules were located under a dissecting microscope, dissected in a cube of agar, dehydrated in a graded series of alcohol, and processed in Lowicryl K4M. The tubules were oriented to the extent possible parallel to the block face to maximize the number of cell profiles included in each ultrathin section. Samples were polymerized under ultraviolet light as described previously.[41] Ultrathin sections were cut and labeled for pendrin and the H^+-ATPase using the anti-pendrin antibody at 1:1000 and the anti–H^+-ATPase antibody at 1:2000 and detection methods described previously.[41]

Quantitative Immunoelectron Microscopic Analysis of Perfused Tubules

Apical plasma membrane boundary length, cytoplasmic area, and pendrin and/or H^+-ATPase immunogold labeling along the plasma membrane and over the cytoplasm, including cytoplasmic vesicles, were quantified in A- and B-IC.[41,42] Every relevant IC in each tubule (*i.e.*, every B cell positive for apical plasma membrane pendrin and basolateral plasma membrane H^+-ATPase as well as every A cell pos-

itive for the apical H^+-ATPase) was photographed and analyzed. IC were photographed at a primary magnification of ×5000 and examined at a final magnification of approximately ×18,200. The exact magnification was calculated by using a calibration grid with 1134 lines/mm. Apical and basolateral plasma membrane boundary length and cytoplasmic area were determined by point and intersection counting using the Merz curvilinear test grid and standard stereologic formulas.[42]

Antibodies

The primary polyclonal antibodies recognizing pendrin[6,41] and B_1 subunit of vacuolar type H^+-ATPase,[33] as well as the secondary goat anti-rabbit IgG antibody conjugated to 0.8-nm colloidal gold particles (Aurion UltraSmall gold conjugate; Electron Microscopy Sciences, Ft. Washington, PA),[41] have been reported previously.

Statistical Analyses

All data are presented as means ± SEM. Data from two collections from each tubule were averaged to obtain a single value. Each "*n*" used in the statistical analysis represents data from an individual tubule. Only one tubule was obtained from a single mouse. For testing for statistical significance between two groups, an unpaired *t* test was used. The criterion for statistical significance was $P < 0.05$.

ACKNOWLEDGMENTS

This work was supported by NIH grant DK 52935 (to S.M.W.). V.P. is the recipient of an AHA Postdoctoral Fellowship Award (0525384B).

We thank Dr. Patrice Bouyer (Department of Cellular and Molecular Physiology, Yale University School of Medicine, New Haven, CT) for her help with the CO_2 assay.

DISCLOSURES

None.

REFERENCES

1. Kriz W, Kaissling B: Structural organization of the mammalian kidney. In: *The Kidney: Physiology and Pathophysiology*, 3rd Ed., edited by Seldin DW, Giebisch G, Philadelphia, Lippincott Williams & Wilkins, 2000, pp 587–654
2. Reeves WB, Andreoli TE: Sodium chloride transport in the loop of Henle, distal convoluted tubule, and collecting duct. In: *The Kidney: Physiology and Pathophysiology*, 3rd Ed., edited by Seldin DW, Giebisch G, Philadelphia, Lippincott Williams & Wilkins, 2000, pp 1333–1369
3. Schuster VL: Function and regulation of collecting duct intercalated cells. *Annu Rev Physiol* 55: 267–288, 1993
4. Wall SM: Recent advances in our understanding of intercalated cells. *Curr Opin Nephrol Hypertens* 14: 480–484, 2005
5. Alper SL, Natale J, Gluck S, Lodish HF, Brown D: Subtypes of intercalated cells in rat kidney collecting duct defined by antibodies against erythroid band 3 and renal vacuolar H+-ATPase. *Proc Natl Acad Sci U S A* 86: 5429–5433, 1989
6. Royaux IE, Wall SM, Karniski LP, Everett LA, Suzuki K, Knepper MA, Green ED: Pendrin, encoded by the Pendred syndrome gene, resides in the apical region of renal intercalated cells and mediates bicarbonate secretion. *Proc Natl Acad Sci U S A* 98: 4221–4226, 2001
7. Soleimani M, Greeley T, Petrovic S, Wang Z, Amlal H, Kopp P, Burnham CE: Pendrin: An apical Cl−/OH-/HCO3− exchanger in the kidney cortex. *Am J Physiol Renal Physiol* 280: F356–F364, 2001
8. Kim YH, Kwon TH, Frische S, Kim J, Tisher CC, Madsen KM, Nielsen S: Immunocytochemical localization of pendrin in intercalated cell subtypes in rat and mouse kidney. *Am J Physiol Renal Physiol* 283: F744–F754, 2002
9. Teng-umnuay P, Verlander JW, Yuan W, Tisher CC, Madsen KM: Identification of distinct subpopulations of intercalated cells in the mouse collecting duct. *J Am Soc Nephrol* 7: 260–274, 1996
10. Schuster VL, Stokes JB: Chloride transport by the cortical and outer medullary collecting duct. *Am J Physiol* 253: F203–F212, 1987
11. Stoner LC, Burg MB, Orloff J: Ion transport in cortical collecting tubule: Effect of amiloride. *Am J Physiol* 227: 453–459, 1974
12. Pech V, Kim YH, Weinstein AM, Everett LA, Pham TD, Wall SM: Angiotensin II increases chloride absorption in the cortical collecting duct in mice through a pendrin-dependent mechanism. *Am J Physiol Renal Physiol* 292: F914–F920, 2007
13. Verlander JW, Kim YH, Shin W, Pham TD, Hassell KA, Beierwaltes WH, Green E, Everett LA, Matthews SW, Wall SM: Dietary Cl− restriction upregulates pendrin expression within the apical plasma membrane of type B intercalated cells. *Am J Physiol Renal Physiol* 291: F833–F839, 2006
14. Verlander JW, Hassell KA, Royaux IE, Glapion DM, Wang ME, Everett LA, Green ED, Wall SM: Deoxycorticosterone upregulates PDS (Slc26a4) in mouse kidney: Role of pendrin in mineralocorticoid-induced hypertension. *Hypertension* 42: 356–362, 2003
15. Valles P, Wysocki J, Batlle D: Angiotensin II and renal tubular ion transport. *Sci World J* 5: 680–690, 2005
16. Wagner CA, Finberg KE, Breton S, Marshansky V, Brown D, Geibel JP: Renal vacuolar H+-ATPase. *Physiol Rev* 84: 1263–1314, 2004
17. Na KY, Oh YK, Han JS, Joo KW, Lee JS, Earm JH, Knepper MA, Kim GH: Upregulation of Na+ transporter abundances in response to chronic thiazide or loop diuretic treatment in rats. *Am J Physiol Renal Physiol* 284: F133–F143, 2003
18. Quentin F, Chambrey R, Trinh-Trang-Tan MM, Fysekidis M, Cambillau M, Paillard M, Aronson PS, Eladari D: The Cl−/HCO3− exchanger pendrin in the rat kidney is regulated in response to chronic alterations in chloride balance. *Am J Physiol Renal Physiol* 287: F1179–F1188, 2004
19. Kovacikova J, Winter C, Loffing-Cueni D, Loffing J, Finberg KE, Lifton RP, Hummler E, Rossier B, Wagner CA: The connecting tubule is the main site of the furosemide-induced urinary acidification by the vacuolar H+-ATPase. *Kidney Int* 70: 1706–1716, 2006
20. Navar LG, Nishiyama A: Why are angiotensin concentrations so high in the kidney? *Curr Opin Nephrol Hypertens* 13: 107–115, 2004
21. Jentsch TJ: Chloride transport in the kidney: Lessons from human disease and knockout mice. *J Am Soc Nephrol* 16: 1549–1561, 2005
22. Emmons C, Stokes JB: Cellular actions of cAMP on HCO3(-)-secreting cells of rabbit CCD: Dependence on in vivo acid-base status. *Am J Physiol* 266: F528–F535, 1994
23. Wagner CA, Giebisch G, Lang F, Geibel JP: Angiotensin II stimulates vesicular H+-ATPase in rat proximal tubular cells. *Proc Natl Acad Sci U S A* 95: 9665–9668, 1998
24. Barreto-Chaves ML, Mello-Aires M: Effect of luminal angiotensin II and ANP on early and late cortical distal tubule. *Am J Physiol* 271: F977–F984, 1996
25. Oliveira-Souza M, Malnic G, Mello-Aires M: Atrial natriuretic peptide impairs the stimulatory effect of angiotensin II on H+-ATPase. *Kidney Int* 62: 1693–1699, 2002

26. Tojo A, Tisher CC, Madsen KM: Angiotensin II regulates H(+)-ATPase activity in rat cortical collecting duct. *Am J Physiol* 267: F1045–F1051, 1994
27. Peti-Peterdi J, Warnock DG, Bell PD: Angiotensin II directly stimulates ENaC activity in the cortical collecting duct via AT(1) receptors. *J Am Soc Nephrol* 13: 1131–1135, 2002
28. Star RA, Burg MB, Knepper MA: Bicarbonate secretion and chloride absorption by rabbit cortical collecting ducts: Role of chloride/bicarbonate exchange. *J Clin Invest* 76: 1123–1130, 1985
29. Dossena S, Maccagni A, Vezzoli V, Bazzini C, Garavaglia ML, Meyer G, Furst J, Ritter M, Fugazzola L, Persani L, Zorowka P, Storelli C, Beck-Peccoz P, Botta G, Paulmichl M: The expression of wild-type pendrin (SLC26A4) in human embryonic kidney (HEK 293 Phoenix) cells leads to the activation of cationic currents. *Eur J Endocrinol* 153: 693–699, 2005
30. Tomita K, Pisano JJ, Knepper MA: Control of sodium and potassium transport in the cortical collecting duct of the rat: Effects of bradykinin, vasopressin, and deoxycorticosterone. *J Clin Invest* 76: 132–136, 1985
31. Gluck S, Al-Awqati Q: An electrogenic proton-translocating adenosine triphosphatase from bovine kidney medulla. *J Clin Invest* 73: 1704–1710, 1984
32. Koeppen BM, Helman SI: Acidification of luminal fluid by the rabbit cortical collecting tubule perfused in vitro. *Am J Physiol* 242: F521–F531, 1982
33. Kim YH, Verlander JW, Matthews SW, Kurtz I, Shin W, Weiner ID, Everett LA, Green ED, Nielsen S, Wall SM: Intercalated cell H+/OH-transporter expression is reduced in Slc26a4 null mice. *Am J Physiol Renal Physiol* 289: F1262–F1272, 2005
34. Milton AE, Weiner ID: Regulation of B-type intercalated cell apical anion exchange activity by CO2/HCO3−. *Am J Physiol* 274: F1086–F1094, 1998
35. Wall SM, Kim YH, Stanley L, Glapion DM, Everett LA, Green ED, Verlander JW: NaCl restriction upregulates renal Slc26a4 through subcellular redistribution: Role in Cl− conservation. *Hypertension* 44: 982–987, 2004
36. Drose S, Altendorf K: Bafilomycins and concanamycins as inhibitors of V-ATPases and P-ATPases. *J Exp Biol* 200: 1–8, 1997
37. Zhou Y, Bouyer P, Boron WF: Role of a tyrosine kinase in the CO2-induced stimulation of HCO3− reabsorption by rabbit S2 proximal tubules. *Am J Physiol Renal Physiol* 291: F358–F367, 2006
38. Taniguchi J, Tsuruoka S, Mizuno A, Sato J, Fujimura A, Suzuki M: TRPV4 as a flow sensor in flow-dependent K+ secretion from the cortical collecting duct. *Am J Physiol Renal Physiol* 292: F667–F673, 2007
39. Knepper MA, Good DW, Burg MB: Ammonia and bicarbonate transport by rat cortical collecting ducts perfused in vitro. *Am J Physiol* 249: F870–F877, 1985
40. Knepper MA, Good DW, Burg MB: Mechanism of ammonia secretion by cortical collecting ducts of rabbits. *Am J Physiol* 247: F729–F738, 1984
41. Wall SM, Hassell KA, Royaux IE, Green ED, Chang JY, Shipley GL, Verlander JW: Localization of pendrin in mouse kidney. *Am J Physiol Renal Physiol* 284: F229–F241, 2003
42. Weibel ER, Bolender RP: Stereological techniques for electron microscopic morphometry. In: *Principles and Techniques of Electron Microscopy*, edited by Hayat MA, New York, Van Nostrand Reinhold Co. Ltd.; 1973, pp 237–296